 doi:10.20944/preprints202210.0322.v1

Article

Automatic Center Detection of Tropical Cyclone using Image Processing based on the Operational Radar Network

Sun-Jin Mo and Ji-Young Gu*

Weather Radar Center of Korea Meteorological Administration, Seoul 07062, Korea; mosunjin@korea.kr
* Correspondence: guji920@korea.kr; Tel.: +82-2-2181-0872

Abstract: This study presents the algorithm ACTION, defined as Automatic Center detection of Tropical cyclone (TC) using Image processing based on the Operational radar Network. Based on the high visibility of weather radar imagery, the TC's motion vector is calculated from the continuous image change using optical flow, producing its rotation center as the TC's center. The algorithm's performance was verified for typhoons (TCs in the Northwestern Pacific) affecting the Korean Peninsula from 2018–2021 and showed a high detection rate of 80.8% within an error distance of 40 km compared to the best track of the Korea Meteorological Administration (KMA). The detection rate was 100% for typhoons with temporally consistent morphological characteristics. ACTION automatically generates TC center information upon the TC's initial entry inside the observation radius even in the absence of uniform radar data. ACTION easily calculates using Open Source Computer Vision, performs in real time, and can be directly applied to rapidly generated weather radar images; hence, it is currently being utilized by the KMA. The high-temporal-resolution TC center information calculated through ACTION is expected to improve the efficiency of TC forecasting.

Keywords: TC center detection; image processing; optical flow; operational radar network; ACTION

1. Introduction

Tropical cyclones (TCs) are one of the world's most dangerous weather phenomena, causing property damage and loss of lives. TCs are driven by complex air–sea interactions and are developed as low-pressure systems over the tropical oceans with intense warm-cored cyclonic vortices [1]. Accurate and rapid analysis of the TC central location is crucial for disaster mitigation. It is essential to analyze the intensity and forecast the path of TCs [2, 3], such to provide rapidly updated information for issuing TC warnings as early as possible.

Although many forms of meteorological data are collected automatically, TC center determination is often conducted manually. The TC center information, which does not sufficiently exclude the subjectivity of the analysis, may show an error of about 0.3° depending on forecaster error [4]. Many TC center automatic detection methods are based on satellite data [5–7]. However, in the case of utilizing weather radar as an observation network, better results should be expected because this approach has an observation range that can sufficiently monitor TCs with high spatial and temporal resolution. Furthermore, weather radar is useful for monitoring dangerous weather phenomena not only because of its high-density data, but also owing to the high visibility of radar images. Considering the visibility advantage of radar images, image processing methods can be applied to them. In particular, TCs can be easily analyzed with such methods because the characteristics of TC movement can be used as key signals in the image processing techniques.

In the context of manual or semiautomatic TC center analysis using radar data, automatic estimation of the TC center through image processing methods using radar images

Preprints (www.preprints.org) | NOT PEER-REVIEWED | Posted: 21 October 2022 doi:10.20944/preprints202210.0322.v1

is a novel approach. One of the standard image processing methods for computing motion vectors is optical flow. The main idea of the optical flow method is to derive motion vectors from the differences of subsequent images. Operational weather radar images are usually produced every 10 min or less, hence the differences of radar images can be calculated by comparing at these intervals. Then, from the image differences, a motion vector field can be calculated. This vector may contain some actual TC movement components, but it cannot be said to represent 100% of the TC movement or atmospheric flow around the TC. However, the vector derived from the instantaneous change in the radar image is an important clue to detect the full change in the movement of the TC, and if the TC is continuously tracked, information on its movement path can be confirmed.

Multiple methods have been used for TC center detection, and their main concepts can be broadly classified into four categories. The first is to determine the geometrical characteristics of the TC [8]; the second is to determine if the wind speed at the center of the TC is zero [9, 10]; the third is to detect the dynamic center using features such as pressure, position elevation, and stream function [11, 12]; and finally, the fourth is to detect the maximum circulation of the TC center [13]. In this study, we introduce a method utilizing the concept of locating the maximum circulation point of the TC center using a motion vector field derived from changes between radar images. The derived vector field is performed through computer image processing in which the forecaster selects the center point of rotation of the TC as the center of the TC in the radar echo image, minimizing the subjectivity of TC analysis through the radar image among forecasters. Our proposed algorithm is the Automatic Center detection of Tropical cyclone using Image processing based on Operational radar Network, abbreviated as ACTION. ACTION is intended to expand the various fields of the application of radar utilizing the visibility of radar imagery.

2. Materials and Methods

2.1. Optical flow technique

The main function of ACTION is to calculate the center of rotation, which characterizes the location of the TC, by extracting the visible changes in radar echo images. To extract the image changes, the optical flow technique is widely used. Optical flow attempts to calculate the motion between two image frames which are taken at times t and $t+\Delta t$ at every pixel position. In this technique, pixel intensities of an object are assumed as constant between consecutive image frames. The change of pixel location (x, y, t) with intensity $I(x, y, t)$ will have changed by Δx, Δy, and Δt between the two image frames. This relationship is described by Eq. (1):

$$I(x, y, t) = I(x + \Delta x, y + \Delta y, t + \Delta t) \tag{1}$$

Assuming the movement is very small, the intensity $I(x, y, t)$ can be understood as flows with Taylor series, as shown in Eq. (2):

$$I(x + \Delta x, y + \Delta y, t + \Delta t) = I(x, y, t) + (\partial I/\partial x)\Delta x + (\partial I/\partial y)\Delta y + (\partial I/\partial t)\Delta t + \cdots \tag{2}$$

By truncating the higher order terms and dividing by Δt, the optical flow equation can be expressed as Eq. (3), where $u=dx/dt$, and $v=dy/dt$:

$$(\partial I/\partial x)u + (\partial I/\partial y)v + (\partial I/\partial t) = 0 \tag{3}$$

In this equation, $\partial I/\partial x$ and $\partial I/\partial y$ can be calculated using image gradients. Similarly, $\partial I/\partial t$ is the gradient according to time. However, u and v are unknown variables that cannot be solved for by using only one equation. Several methods have been provided to solve this type of problem, including Gunner Farneback's algorithm [14], which is based on polynomial expansion. Farneback's method approximates the windows of image frames by quadratic polynomials through polynomial expansion transformation, then, the displacement fields from polynomial expansion coefficients are defined by observing how

Preprints (www.preprints.org) | NOT PEER-REVIEWED | Posted: 21 October 2022 doi:10.20944/preprints202210.0322.v1

the polynomial transforms under motion. The algorithm computes dense optical flow under the assumption of a slowly varying displacement field. This dense optical flow is understood to be very suitable for calculating the displacement field of a radar image containing small changes on the scale of 5 or 10 min, which is the target derivation scale used in this study. In particular, OpenCV (Open Source Computer Vision) provides a tool to easily calculate optical flow, and through this, even non-image processing experts can calculate the motion vector based on the radar image. In this study, the Python function "cv2.calcOpticalFlowFarneback" was used in the programming environment to achieve this. Its default parameters are "flow = cv2.calcOpticalFlowFarneback(prev, next, flow, pyr_scale, levels, winsize, iterations, poly_n, poly_sigma, flags)." The function was executed as "flow = cv2.calcOpticalFlowFarneback(prev, next, flow, pyr_scale=0.5, levels=3, winsize=15, iterations=10, poly_n=10, poly_sigma=1.2, flags=0)." The set values were adjusted and used appropriately according to each research environment.

The role of each parameter in the OpenCV function is as follows: prev is the first input image; next is the second input image of the same type and size as prev; pyr_scale specifies the image scale; levels specifies the image layer; winsize is the averaging window size; iterations specifies the number of iterations to be performed at each level; poly_n designates the size of the pixel neighborhood used to find polynomial expansion for each pixel; poly_sigma is the Gaussian standard deviation used to smooth derivatives for the polynomial expansion; flow is the computed flow image that has a similar size and type as prev; and "flags" indicates the operation flags (the function used cv2.OPTFLOW_FARNEBACK_GAUSSIAN).

2.2. Radar image preprocessing

To use the optical flow technique, three conditions must be met: constancy of image brightness, temporal persistence, and spatial consistency. Based on the radar characteristics that produce data from a fixed observation point at regular time intervals, the temporal persistence and spatial consistency factors can be sufficiently satisfied. However, maintaining the constancy of image brightness is more challenging. Fortunately, radar reflectivity data is expressed as a one-dimensional size value, hence when the radar image is converted to grayscale using this value, the brightness constancy can be satisfied.

The radar image used in this study is a composite of radar data observed from the S-band radar network of the Korea Meteorological Administration (KMA). In particular, the reflectivity composite field expressed as a one-dimensional size value was used, and as described above, it was converted to grayscale for the optical flow calculation. Since the radar composite field is uniformly calculated at 5- or 10-min intervals, temporal persistence can be adjusted easily. Although the radar composite image area is constant according to the radar observation characteristics that perform constant radius observation, a specific window setting was required to improve the computational efficiency and to focus more on the observation of the TC flow, which is the main target in this study. Therefore, an approximate TC area of 500 × 500 km was extracted using the TC prediction path. Although the possibility of a sudden change in the predicted path of a TC cannot be excluded, there are no records of a TC moving 500 km within 5 or 10 min, thus the selection of an appropriate optical flow calculation region using the central position of the TC center calculated in the previous frame is sufficient.

2.3. ACTION methodology

Weather radar data is composed of multiple variables, including reflectivity, radial velocity, and differential reflectivity and differential phase shift, which are dual polarization variables. It is possible to comprehend the physical meaning of the precipitation system using these variables. However, the biggest advantage of weather radar data is that it provides visual information about weather phenomena with high spatiotemporal resolution. The main feature of the ACTION algorithm is that it directly utilizes radar imagery.

Preprints (www.preprints.org) | NOT PEER-REVIEWED | Posted: 21 October 2022 doi:10.20944/preprints202210.0322.v1

In the algorithm, the motion vector is extracted using the optical flow of the change between consecutive radar images. ACTION is largely divided into four steps: (i) valid vector field calculation, (ii) dense vector field generation, (iii) TC rotation component extraction, and (iv) TC center selection.

2.3.1. Valid vector field calculation

In the first step, basic motion vectors are extracted from continuous radar images through the optical flow technique. Since optical flow is not intended to extract meteorologically meaningful vector fields, it is necessary to filter out vectors with little meteorological significance. Motion vectors are considered to be lacking in meteorological significance when one of u and v components has a value of 0. Of course, it is possible for an atmospheric flow to exist with predominant u and v components, but in meteorological terms, it is extremely rare that such a single u, v value would persist above a certain scale.

Considering resolution, if the resolution is set too small, it may cause the generation of inhomogeneous vectors with large errors as well as the generation of unusual u and v vectors. Using the dataset for a total of 14 typhoons that affected the Korean Peninsula between 2018 and 2021 (Table 1), it was confirmed that the error size of the inhomogeneous vector generated according to the change in resolution increased linearly with an increase in resolution (Figure 1). Motion vectors produced through the optical flow technique were delineated by detecting changes in pixels of the image. If the resolution is too dense, it may be difficult to extract the continuity characteristics of the vector. Therefore, it is very important to set an appropriate resolution according to the size of the area of analysis and the characteristics of the object to be analyzed. Figure 2 shows the number of pixels in the analysis field according to the resolution, the unusual u, v vector inclusion ratio, and the time required to create the vector intersection of each pixel when setting the TC center in this algorithm. A resolution of 40 km was determined to be an appropriate window size by considering the vector intersection creation time of 30 seconds or less, the number of at least 100 windows required for vector calculation, and the ratio containing the least abnormal u and v vectors when utilizing this algorithm.

Table 1. List of typhoons that affected the Korean Peninsula between 2018–2021.

No.	Typhoon	Year	Period
1	PRAPIROON	2018	Jun 29–Jul 4
2	SOULIK	2018	Aug 16–25
3	KONG-REY	2018	Sep 29–Oct 7
4	DANAS	2019	Jul 16–20
5	FRANCISCO	2019	Aug 2–6
6	LINGLING	2019	Sep 2–8
7	TAPAH	2019	Sep 19–23
8	MITAG	2019	Sep 28–Oct 3
9	JANGMI	2020	Aug 9–10
10	BAVI	2020	Aug 22–27
11	MAYSAK	2020	Aug 28–Sep 3
12	HAISHEN	2020	Sep 1–7
13	OMAIS	2021	Aug 20–24
14	CHANTHU	2021	Sep 7–18

Preprints (www.preprints.org) | NOT PEER-REVIEWED | Posted: 21 October 2022 doi:10.20944/preprints202210.0322.v1

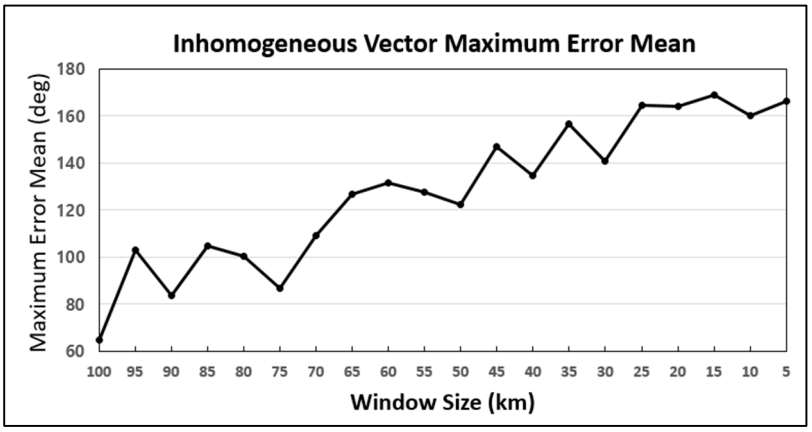

Figure 1. Inhomogeneous vector maximum error mean according to resolution changes of the motion vector calculation for 14 typhoon cases from 2018 to 2021.

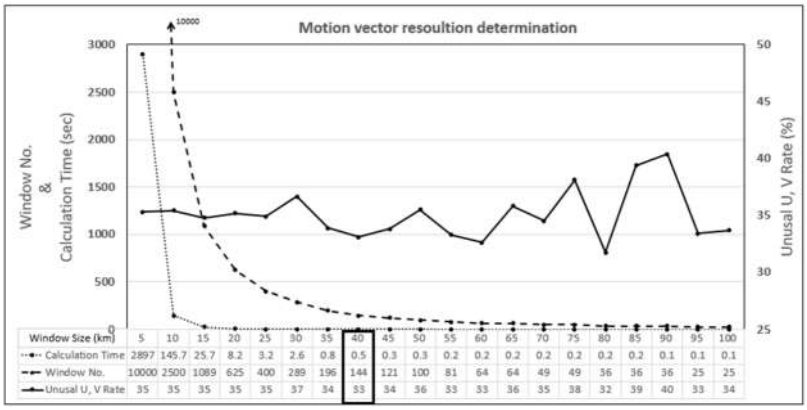

Figure 2. The calculation time (small dotted line) required to create the vector intersection of each pixel, the number of windows (thick dotted line) in the analysis field, and the unusual u and v vector generation rate (solid line) according to resolution (window size) when running the ACTION algorithm. Appropriate resolution selection conditions (black-outlined data) suitable for motion vector generation(computation time 30 seconds or less, number of windows 100 or more, minimum abnormal u and v vector generation rate).

Since the motion vector can be calculated only in the region where the radar echo image exists, it is necessary to determine the total airflow required to derive the rotation component, which is a key factor for finding the center of the TC. In particular, if there is no radar echo and there is a high percentage of vector blank areas, which are areas where vectors are not calculated, the accuracy of the TC center selection may be reduced. To minimize this problem in the algorithm, some vector blank areas of the radar echo proximity region are linearly interpolated using the neighboring vector data. The valid vector field is finally calculated by removing a single u, v vector and averaging with the previous motion vector field generated in the previous time. Figure 3 shows the radar composite image of the 8th typhoon "BAVI" case at 14:00 KST August 26, 2020. The red box is the area selected to calculate the valid vector field, and this area is continuously updated over time based on the TC center position selected according to the operation of the ACTION algorithm. Figure 4(a) is the basic motion vector calculation and 4(b) is the valid vector field.

Preprints (www.preprints.org) | NOT PEER-REVIEWED | Posted: 21 October 2022 doi:10.20944/preprints202210.0322.v1

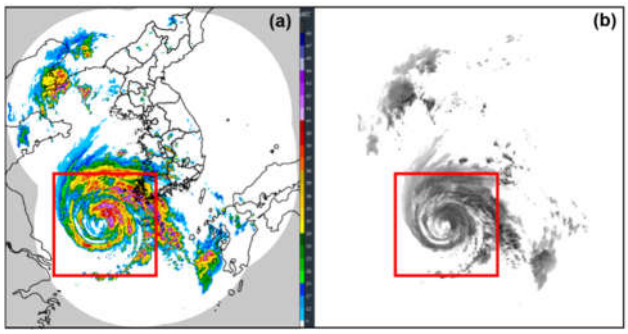

Figure 3. (**a**) Radar reflectivity and (**b**) grayscale converted composite images of the 8th typhoon case named "BAVI", at 14:00 KST on August 26, 2020. The red boxes denote the valid vector calculation areas (500 × 500 km) used in the ACTION algorithm.

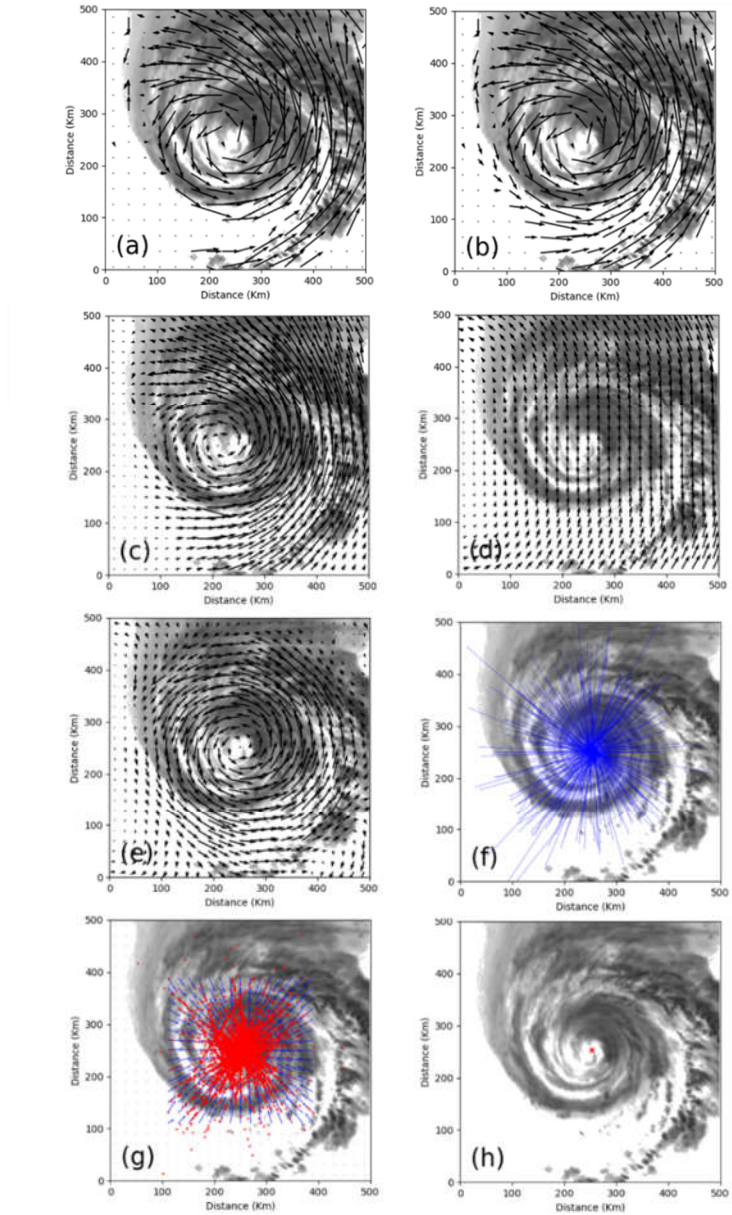

Figure 4. ACTION algorithm process: (**a**) Basic motion vector calculation, (**b**) valid vector field calculation, (**c**) generating a dense vector field, (**d**) background airflow extraction, (**e**) TC rotation component extraction, (**f**) creating a tangential intersection of rotation components, (**g**) calculating maximum density of intersections, and (**h**) selecting the TC center.

Preprints (www.preprints.org) | NOT PEER-REVIEWED | Posted: 21 October 2022 doi:10.20944/preprints202210.0322.v1

2.3.2. Generating the dense vector field

As described above, among the methods of selecting the TC center using radar data, the approach used in this study is to determine the maximum circulation of the TC center. In order to more precisely grasp the rotational flow of the TC, it is necessary to upscale the vector resolution and interpolate far empty spots other than the area having radar echo. To create such a dense vector field, the resolution was increased from 40 to 20 km, and the vector empty area was interpolated using the radial basis function (RBF) to generate the dense motion vector field for the entire analysis field. Mathematically, the radial function is defined as a function of the distance from the origin to each point in the Euclidean space, so the RBF interpolation has the advantage of performing smooth interpolation in all areas while maintaining the dominant vector flow characteristics as much as possible. Figure 4(c) shows the dense vector field calculated through resolution upscaling and RBF interpolation. As can be seen in the figure, a dense and smooth vector field was produced while maintaining the dominant vector characteristics, which made it possible to perform the subsequent background field removal and rotational component extraction more efficiently.

2.3.3. Extracting the rotation component of TC

The center of a TC can be regarded as a morphologically strong center of rotation. From a meteorological point of view, it is also necessary to determine the TC center based on meteorological data such as air pressure and wind, but the purpose of this study was to focus only on the automatic selection of the TC centers using radar image data itself. In order to extract only the rotation component of the TC the mean flow component of the entire analysis field should be separated and removed. To achieve this in this study, the mean flow vector was obtained by calculating the average of the vectors while moving a window of a certain size at the analysis field, and 20 pixels was set as the moving window. Figure 4(d) shows the mean flow vector of the analyzed field calculated in this way, and Figure 4(e) illustrates the extraction of the rotation component of the TC by removing the mean flow vector. In the rotation vector field of the TC derived in this way, the center can be selected as the convergence region of the rotation vector normal with consideration to the centripetal force principle of rotation.

2.3.4. Selecting the TC center

The center of the TC is determined in the ACTION algorithm by finding the convergence point of centripetal force, which is a virtual force acting in the direction of the center of rotation. With consideration to the counterclockwise rotation (in the northern hemisphere) of the TC an imaginary line segment of 90° is produced counterclockwise, and a length weight is applied to the normal to create intersection points. In this study, the weight of 30 was set in consideration of three items: the spatial resolution of the TC rotation component vector field of 20 km, the computing environment in which the algorithm is operated, and the calculation time. This weight can be appropriately adjusted according to the size of the analysis field to be analyzed, and the conditions of the computing environment. Figure 4(f) shows the generation of intersection points of normal line segments to which the length weight is applied.

Finally, in the last step of the ACTION algorithm, the maximum density point among the intersection points is determined as the center of the TC. To establish the maximum density point, kernel density estimation (KDE) is used for this. The KDE technique compensates for the bin discontinuity of the two-dimensional histogram technique, which is usually the simplest form of density estimation, and has the advantage of obtaining a smooth-shaped probability density function. However, appropriate functions for efficient calculation and resolution of analysis data can be derived only by setting appropriate bin size and band width. In this study, the bin size was set to 100 and the band width was set to 1. Figure 5 shows an example of selecting the maximum density of the rotation vector

Preprints (www.preprints.org) | NOT PEER-REVIEWED | Posted: 21 October 2022 doi:10.20944/preprints202210.0322.v1

normal intersection using the two-dimensional histogram and KDE technique, respectively, by applying the ACTION algorithm to the 5th typhoon case called "DANAS," which occurred at 12:00 KST on July 20, 2019.

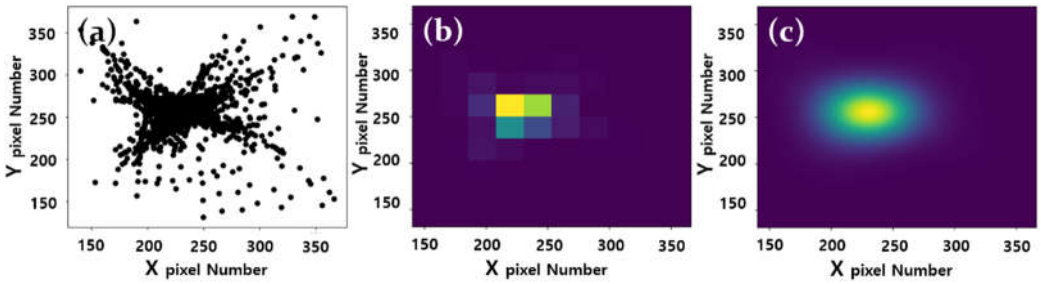

Figure 5. An example of the maximum density selection of (a) intersection points of the rotation vector normal lines using the (b) two-dimensional histogram and (c) kernel density function technique on the 5th typhoon case called "DANAS," at 12:00 KST on July 20, 2019.

3. Results

In order to evaluate the performance of the ACTION algorithm, a total of 14 typhoons that affected the Korean Peninsula between 2018 and 2021 were analyzed (Table 1). Radar images of the lowest elevation angle radar reflectivity plan position indicator with 480 km were used. Since 2020, the radar observation time has been improved from 10 to 5 min, thus, radar images at 10-min intervals during 2018–2019 and 5-min intervals during 2020–2021 were used for the evaluation. For each typhoon, the track generated by ACTION was compared to the corresponding best track data determined by the KMA based on ground meteorological data after the typhoon passed the Korean Peninsula.

3.1. Performance of the ACTION algorithm

The biggest advantage of ACTION is that even when only a few radar echoes are present in the analysis area, it is still possible to detect small changes in the echoes and extract the central information of the TC. Figures 6 and 7 show composite images of radar reflectivity for cases in which typhoons that affected the Korean Peninsula during 2018–2021 clearly showed their morphological characteristics. When selecting the center of a TC based on radar data, in the case of the methods using the TC geometry [15] or radar radial velocity information [10, 16], it is typically difficult to calculate sufficient information if the radar echo itself is not sufficient. If the radar echo information is insufficient when the TC begins to enter the radar observation radius, or if its intensity is weakened after landing on the ground, the accuracy of the TC center information by these methods is likely to decrease. However, by using ACTION, even when the geometrical characteristics of the TC are not clear (Figs. 6(e), 6(g), and 7(a)), it is possible to detect the radar echo flow changes in the analysis area and calculate the TC center information. As shown by the data listed in Table 2, ACTION results had an average detection rate of 80.8% within an error distance of 40 km for all 14 typhoons that were evaluated in this study. Among them, "JANGMI" and "HAISHEN," whose morphological rotation was relatively well maintained in the typhoon's movement path, showed a detection rate of 100% within an error distance of 40 km.

 doi:10.20944/preprints202210.0322.v1

Table 2. Detection rate by error distance of ACTION results for typhoons that affected the Korean Peninsula between 2018–2021.

No.	Typhoon	Year	Detection rate within ** error distance (%)				
			**40 km	**30 km	**20 km	**10 km	**5 km
1	PRAPIROON	2018	56.6	35.7	16.3	3.1	0.0
2	SOULIK	2018	87.8	72.3	33.5	8.6	2.5
3	KONG-REY	2018	76.6	48.7	25.2	9.0	0.9
4	DANAS	2019	83.2	61.8	31.5	7.9	1.1
5	FRANCISCO	2019	87.4	54.0	25.3	5.8	1.2
6	LINGLING	2019	51.8	33.3	13.5	5.0	0.7
7	TAPAH	2019	71.1	51.8	25.3	10.8	2.4
8	MITAG	2019	57.2	29.5	4.6	0.6	0.0
9	JANGMI	2020	100.0	96.6	72.4	27.6	6.9
10	BAVI	2020	88.1	71.9	58.1	21.3	1.3
11	MAYSAK	2020	89.9	83.7	48.8	7.0	0.0
12	HAISHEN	2020	100.0	64.5	26.3	6.6	1.3
13	OMAIS	2021	96.5	72.1	33.7	2.3	0.0
14	CHANTHU	2021	85.3	75.3	54.7	8.0	0.7
	Mean:		**80.8**	**60.8**	**33.5**	**8.8**	**1.4**

Figures 8 and 9 compare the typhoon center calculated by ACTION every 10 min and the typhoon center selected by the KMA every hour for all 14 typhoon cases in the form of a track. In the figures, the red line indicates the typhoon center information calculated by ACTION, and the blue line indicates that selected by the KMA. In Figures 8 and 9, the ACTION results are data at 10-min intervals and show the shaking of the center of the typhoon due to its' rotation (see red lines). On the other hand, since the typhoon center information selected by the KMA is displayed every hour, this fluctuation seems to have been somewhat alleviated (see blue lines). In the case of any given TC, because the movement of the synoptic barometer and rotational motion of the TC itself are highly complex, the center of the TC moves while shaking to some extent. Therefore, the continuous production of TC-centered information is highly useful for determining the boundaries of dangerous weather areas according to the movement of TCs, as well as for producing meteorological information. In the case of using ACTION, it is useful for acquiring TC center location information in areas where direct observation data is difficult to utilize, such as over the open ocean. If the radar data in the observation area is sufficiently filled, it becomes simpler to determine the location of the center of the TC, even in sea areas, using a general radar image. However, as described above, when radar data is not uniformly distributed or when a TC has just entered within the radar observation radius, it is difficult to select a TC center using the characteristics of a general radar image. In this context, the results of ACTION for the 14 typhoon cases in this study are very encouraging.

Preprints (www.preprints.org) | NOT PEER-REVIEWED | Posted: 21 October 2022 doi:10.20944/preprints202210.0322.v1

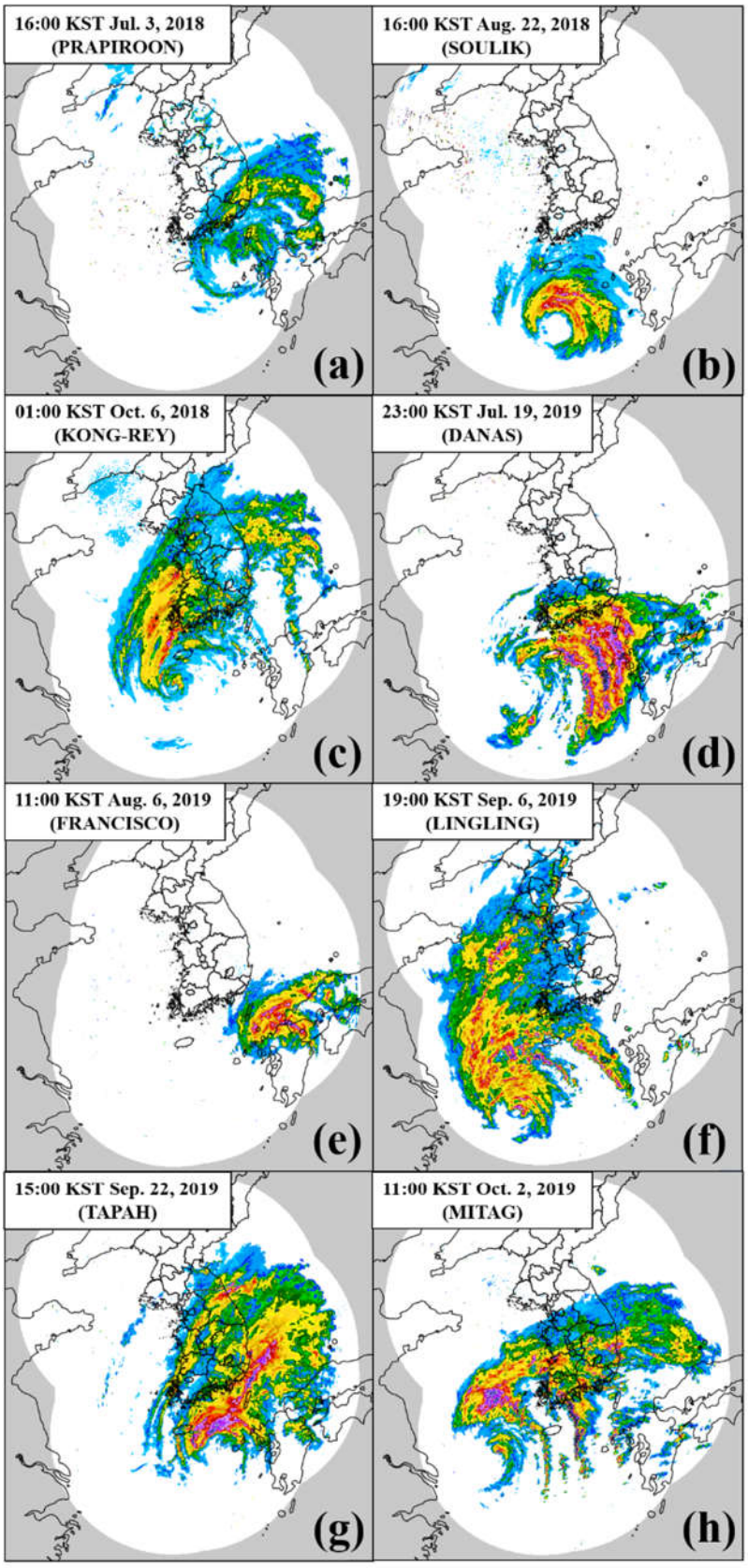

Figure 6. Composite images of radar reflectivity of typhoons that affected the Korean Peninsula between 2018–2019: (**a**) "PRAPIROON," (**b**) "SOULIK," (**c**) "KONG-REY," (**d**) "DANAS," (**e**) "FRANCISCO," (**f**) "LINGLING," (**g**) "TAPAH," and (**h**) "MITAG.".

Preprints (www.preprints.org) | NOT PEER-REVIEWED | Posted: 21 October 2022 doi:10.20944/preprints202210.0322.v1

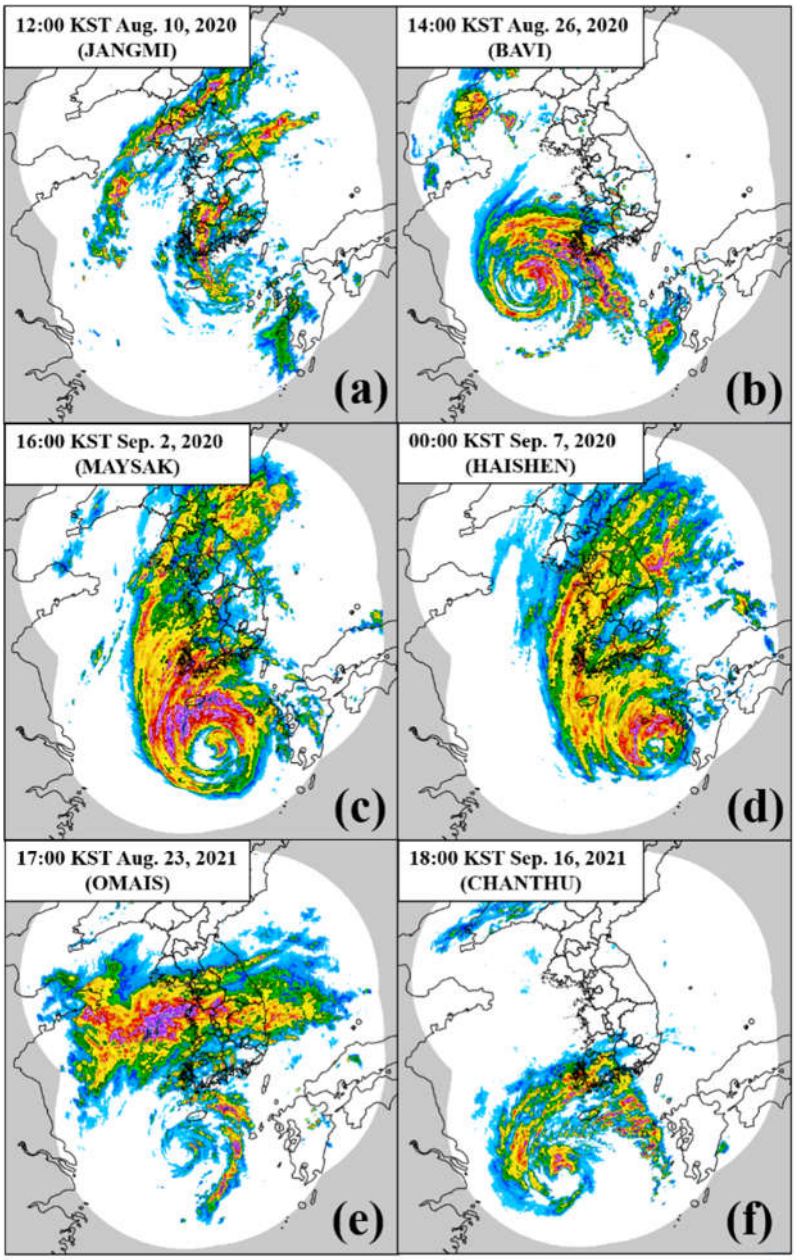

Figure 7. Composite images of radar reflectivity of typhoons that affected the Korean Peninsula between 2020–2021: (**a**) "JANGMI," (**b**) "BAVI," (**c**) "MAYSAK," (**d**) "HAISHEN," (**e**) "OMAIS," and (**f**) "CHANTHU.".

Preprints (www.preprints.org) | NOT PEER-REVIEWED | Posted: 21 October 2022 doi:10.20944/preprints202210.0322.v1

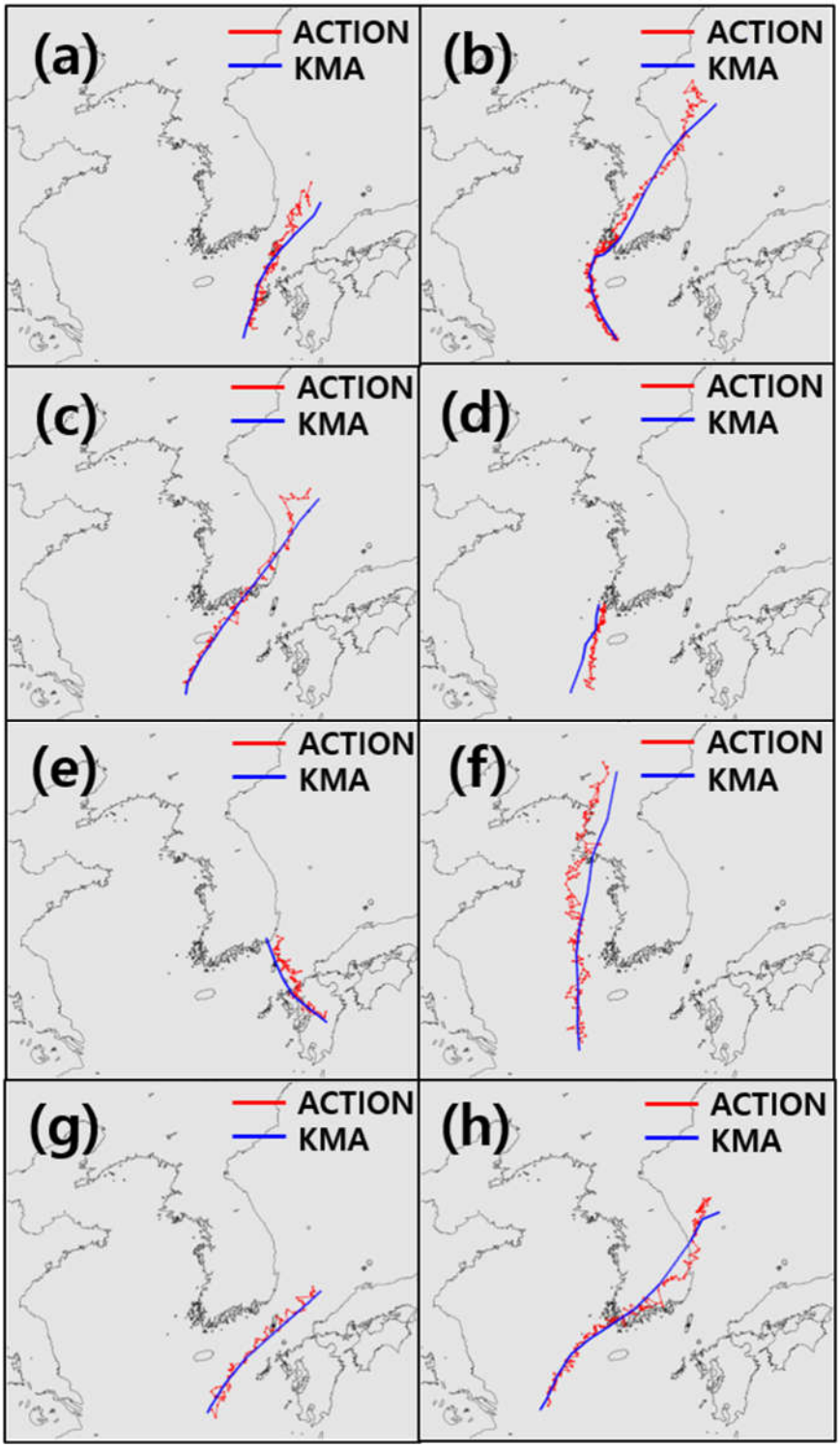

Figure 8. Comparison of ACTION results and KMA best track of typhoons that affected the Korean Peninsula between 2018–2019: (**a**) "PRAPIROON," (**b**) "SOULIK," (**c**) "KONG-REY," (**d**) "DANAS," (**e**) "FRANCISCO," (**f**) "LINGLING," (**g**) "TAPAH," and (**h**) "MITAG.".

Preprints (www.preprints.org) | NOT PEER-REVIEWED | Posted: 21 October 2022 doi:10.20944/preprints202210.0322.v1

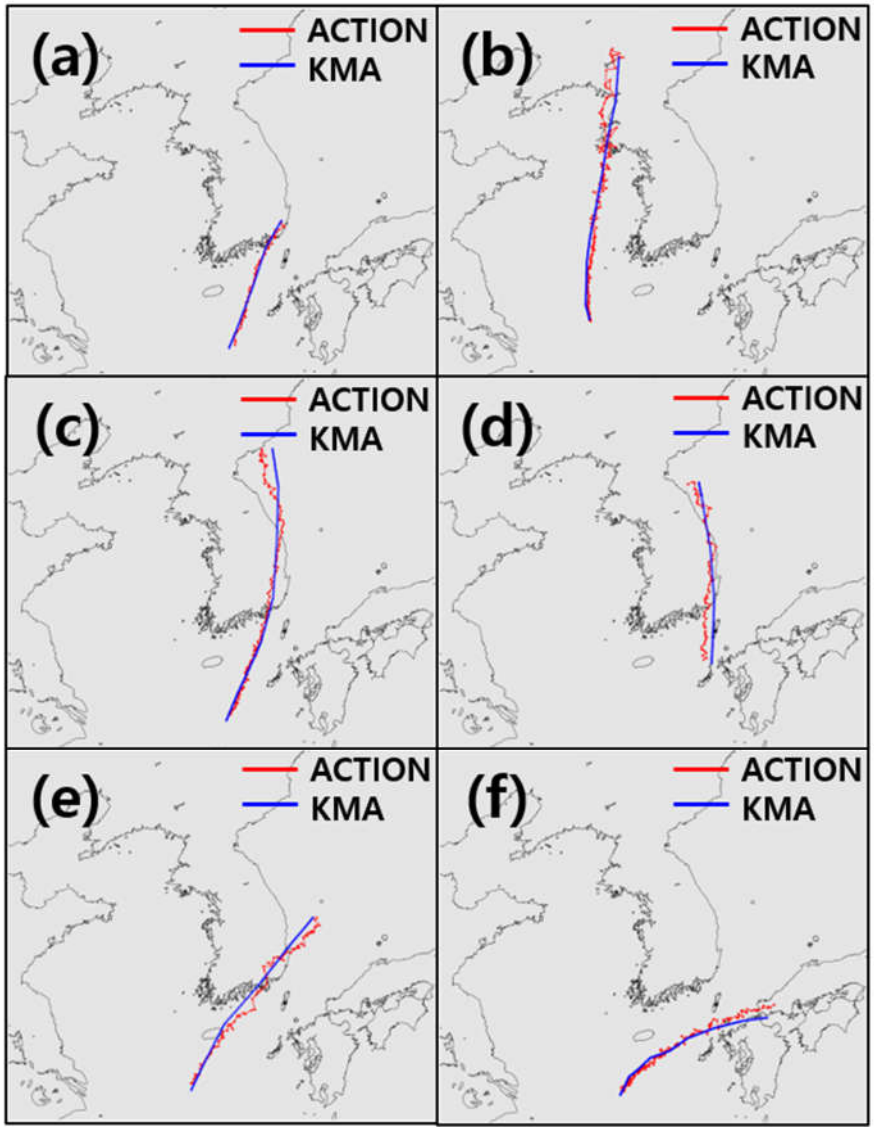

Figure 9. Comparison of ACTION results and KMA best track of typhoons that affected the Korean Peninsula between 2020–2021: (**a**) "JANGMI," (**b**) "BAVI," (**c**) "MAYSAK," (**d**) "HAISHEN," (**e**) "OMAIS," and (**f**) "CHANTHU.".

3.2. Image time interval change effect

As an image processing technique, the basis of ACTION technology is that the shorter the interval between images, the better the performance. This is because if the interval between images is shortened, it is possible to better capture small changes in the images, allowing high-quality motion vectors to be calculated. The Weather Radar Center of the KMA significantly improved their radar composite image generation time from 10 min to 5 min, hence when ACTION was applied, the results showed a noticeable performance improvement. As shown in Table 3, when images were used at 5-min intervals for five typhoons between 2020–2021, the average detection rate improved by 20% within an error distance of 20 to 40 km. When using the 5-min interval, the detection rate was over 85% within an error distance of 40 km, which is sufficient to be used in the TC forecasting field. The acquisition of high-accuracy continuous TC location information enables more accurate dangerous area setting and timely warning delivery in TC forecasting. Therefore, the use of ACTION, which is based on weather radar images with high temporal resolution, contributes to more accurate TC information production.

Preprints (www.preprints.org) | NOT PEER-REVIEWED | Posted: 21 October 2022 doi:10.20944/preprints202210.0322.v1

Table 3. Detection rate by error distance of ACTION results according to radar image interval improvement (from 10 to 5 min) for typhoons that affected the Korean Peninsula between 2020–2021.

Image Interval	Typhoon	Year	Detection rate within ** error distance (%)				
			**40 km	**30 km	**20 km	**10 km	**5 km
10 min	JANGMI	2020	100.0	87.9	58.6	24.1	5.2
	BAVI	2020	65.0	46.9	21.9	7.5	1.9
	MAYSAK	2020	76.0	60.5	21.7	1.6	0.0
	HAISHEN	2020	58.4	29.2	10.1	0.0	0.0
	OMAIS	2021	70.9	47.7	15.1	0.0	0.0
	CHANTHU	2021	78.7	66.0	40.0	6.0	1.3
	Mean:		**74.8**	**56.4**	**27.9**	**6.5**	**1.4**
5 min	JANGMI	2020	100.0	96.6	72.4	27.6	6.9
	BAVI	2020	88.1	71.9	58.1	21.3	1.3
	MAYSAK	2020	89.9	83.7	48.8	7.0	0.0
	HAISHEN	2020	100.0	64.5	26.3	6.6	1.3
	OMAIS	2021	96.5	72.1	33.7	2.3	0.0
	CHANTHU	2021	85.3	75.3	54.7	8.0	0.7
	Mean:		**93.3**	**77.3**	**49.0**	**12.**	**1.7**
Mean of improved detection rates:			**18.5**	**21.0**	**21.1**	**5.6**	**0.3**

3.3. Utilization of ACTION

Since 2018, new research is being enabled by the expansion of the various uses of weather radar imagery through the development of ACTION. It has been recognized as an independent technology through Korean patent registration in 2020, and has been used for forecasting by the KMA since 2021. When a typhoon approaches the Korean Peninsula, as soon as it enters within the usable radar observation radius, ACTION is automatically executed and the relevant information is calculated in real time. Currently, typhoon center information is produced every 10 min using a radar composite image of the Korean Peninsula at 5-min intervals. It is displayed along with the forecasted or selected path of typhoon by the KMA, and the ACTION information is readily available to analysts. This technology obtained a United States patent in 2022 and has been recognized at home and abroad, and is also being used as the basis for a new conceptual weather radar application to obtain real-time information in the field of weather forecasting. Figure 10 illustrates an example of ACTION being operated in real time by the KMA's radar analysis system. The purple squares connected by purple lines indicate the typhoon center positions as derived through ACTION, and the blue circular connecting lines indicate the final typhoon center positions that were selected by the KMA.

Preprints (www.preprints.org) | NOT PEER-REVIEWED | Posted: 21 October 2022 doi:10.20944/preprints202210.0322.v1

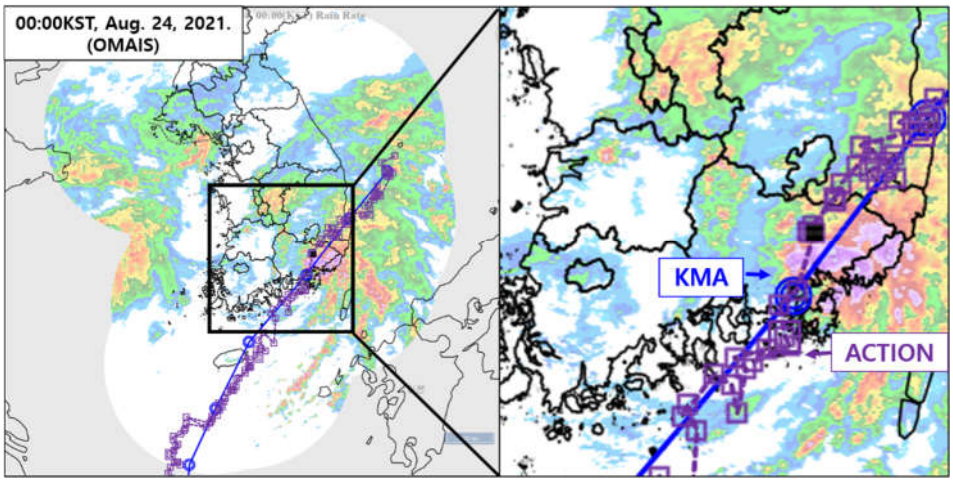

Figure 10. An example of ACTION being operated in real time by the KMA's radar analysis system (typhoon case of "OMAIS," occurring at 00:00 KST, August 24, 2021).

4. Discussion

Most TC center selection studies using existing radar data used data values directly, but in this study, an image processing technique that maximizes the visibility of radar images was applied. Weather radar is a major tool that enables weather forecasters to visually recognize precipitation in the field of weather forecasting, and radar images themselves have a high value in weather forecasting. In addition, the ACTION technology, which quantitatively calculates changes in radar images and uses them for actual prediction, is meaningful. The ACTION, which can identify the movement characteristics of the echo even when many of the TC's typical morphological characteristics have disappeared, can be used in various aspects beyond simply calculating information about the TC. For example, by extracting the movement patterns of a precipitation system at various altitudes, it can be used to determine the characteristics of a three-dimensional precipitation system, and to determine the retention of convective echoes in a specific area by accumulating motion vectors.

However, since the ACTION utilizes change information between radar images, uniform radar images are required at regular intervals. In case of radar failure, intermittent image change can be solved in a short time by inserting the image uniformity check process into this algorithm, but if the range or shape of the radar image changes irregularly over a long period of time, the accuracy of the ACTION results may be reduced. In addition, when the TC landed, if the terrain is high in altitude, such as a mountainous terrain, the radar echo of the lower layer may not follow the actual movement of the TC and may partially stagnate due to the terrain effect. Even in this case, the ACTION results may be slightly less accurate. However, looking at the areas affected by terrain effects differently, we can expect another use of the ACTION technique. In other words, the degree of inclination of the TC can be determined based on the information on the change in the movement of the upper and lower layers of the TC according to the topography. Although not introduced in this paper, meaningful results were confirmed in an experiment to derive the distance and direction difference of the TC center position from the lower radar image and upper radar image. Hopefully, more detailed research results in this field will be introduced in future papers after performing additional validation studies.

The ACTION technique is very affective at using radar images in actual weather forecasting by focusing on the most basic aspects of radar data utilization. Of course, in order to utilize it, uniform output of radar image, sufficient quality control, and detailed setting adjustment according to the computing environment of the institution that wants to implement the technology must be preceded. However, this technology has great significance in that it can enable various uses of weather radar data.

 doi:10.20944/preprints202210.0322.v1

5. Conclusion

The application of the ACTION algorithm can be summarized as follows. ACTION automatically estimates the TC center from operational radar imagery using the optical flow image processing technique. In the algorithm, a motion vector that can explain the flow of a TC is calculated by extracting changes between successive radar images generated at regular time intervals. Gunner Farneback's algorithm [14] is then applied to perform dense vector extraction of each image pixel. In this study, first, the process of converting the operational weather radar composite image produced at intervals of 5 to 10 min into grayscale was carried out to perform ACTION. Then, using the 14 typhoon cases that affected the Korean Peninsula between 2018–2021, an appropriate basic motion vector generation resolution (40 km) was determined by comprehensively considering the computational calculation time and unusual vector calculation rate appropriate for real-time operation. The center of each TC was finally determined through a series of basic motion vector generations, valid vector extraction, dense vector interpolation, background flow field removal, typhoon rotation components extraction, and tangential vector maximum junction generation.

This study verified the performance of ACTION through analysis of the 14 typhoon cases over the Korean Peninsula during 2018–2021. In comparing the ACTION performance results with the best tracks selected by the KMA based on various weather observation data, ACTION showed a high detection rate of 80.8% within an error distance of 40 km. Moreover, the typhoons with well-maintained morphological typhoons showed a 100% detection rate. In this verification process, it was confirmed that the improvement of the time interval (from 10 to 5 min) of the images used in ACTION greatly improved the accuracy of this technique; the performance improved by about 20% within an error distance of 20–40 km.

The biggest advantage of ACTION is its ability to automatically generate central information about a TC even when uniform radar data does not exist within the radar observation radius, or when a TC has just entered within it. In addition, its ability to calculate and utilize new types of information by utilizing the high visibility of radar images beyond the use of radar data itself are very encouraging. We expect that ACTION will contribute to improving the value of weather radar data, in that it produces real-time automatic detection information of the TC center using image processing technology, which is a novel approach in the field of weather radar. This technology has been applied and operated in real time since 2021 by the KMA, and its originality has been recognized by acquiring Korean and United States patents. In the future, based on ACTION technology, we plan to conduct further applied research such as three-dimensional structural analysis of TCs using weather radar images at various altitudes.

6. Patents

Korean patent (Patent Number: 10-2239386), United States patent (Patent Number: US 11,333,795 B2) "**Method for typhoon center automatic selection using vectors calculated from radar image data by optical flow technique, recording medium and device for performing the method**."

Author Contributions: This work was supported by significant contributions from all the authors. Conceptualization, S.-J. Mo and J.-Y. Gu; methodology, S.-J. Mo and J.-Y. Gu; software, S.-J. Mo; validation, S.-J. Mo and J.-Y. Gu; formal analysis, S.-J. Mo and J.-Y. Gu; investigation, J.-Y. Gu; writing—original draft preparation, J.-Y. Gu; writing—review and editing, J.-Y. Gu; visualization, S.-J. Mo and J.-Y. Gu; supervision, J.-Y. Gu; project administration, J.-Y. Gu; funding acquisition, J.-Y. Gu. All authors have read and agreed to the published version of the manuscript.

Funding: This research was supported by the grants "Development of analysis technologies for local-scale weather radar network and next generation radar (KMA2021-03221)" and "Development of radar based severe weather monitoring technology (KMA2021-03121)" of the "Development of integrated application technology for Korea weather radar project" funded by the Weather Radar Center, Korea Meteorological Administration.

Acknowledgments: Authors are very grateful to the members of the Radar Analysis Division, Weather Radar Center for their support of this research and would like to thank Editage (www.editage.co.kr) for English language editing.

Conflicts of Interest: The authors declare no conflict of interest.

References

1. Kepert, J.D. Tropical Cyclone Structure and Dynamics. *World Scientific Series on Asia-Pacific Weather and Climate*; World Scientific Series on Asia-Pacific Weather and Climate, Chan, J.C.L., Kepert, J.D., Eds. **2010**, *4*, 3–53. DOI:10.1142/9789814293488_0001.
2. Wimmers, A.J.; Velden, C.S. Advancements in Objective Multi Satellite Tropical Cyclone Center Fixing. *J. Appl. Meteorol. Climatol.* **2016**, *55*, 197–212. DOI:10.1175/JAMC-D-15-0098.1.
3. Jin, S.; Wang, S.; Li, X.; Jiao, L.; Zhang, J.A.; Shen, D. A Salient Region Detection and Pattern Matching-Based Algorithm for Center Detection of a Partially Covered Tropical Cyclone in a SAR Image. *IEEE Trans. Geosci. Remote Sens.* **2017**, *55*, 280–291.
4. Lam, C.Y. Operational Tropical Cyclone Forecasting from the Perspective of a Small Weather Service. In *Proceedings of the ICSU/WMO International Symposium on Tropical Cyclone Disasters*, Beijing, China, 1992.
5. Dvorak, V.F. Tropical Cyclone Intensity Analysis and Forecasting from Satellite Imagery. *Mon. Wea. Rev.* **1975**, *103*, 420–430. DOI:10.1175/1520-0493(1975)103<0420:TCIAAF>2.0.CO;2.
6. Hasler, A.F.; Palaniappan, K.; Kambhammetu, C.; Black, P.; Uhlhorn, E.; Chesters, D. High Resolution Wind Fields Within the Inner-Core and Eye of a Mature Tropical Cyclone from GOES 1-Min Images. *Bull. Am. Meteor. Soc.* **1998**, *79*, 2483–2496. DOI:10.1175/1520-0477(1998)079<2483:HRWFWT>2.0.CO;2.
7. Wimmers, A.; Velden, C. Satellite-Based Center-Fixing of Tropical Cyclones; New Automated Approaches. In *Proceedings of the 26th Conference on Hurricanes and Tropical Meteorology*, Miami, FL, USA, 2004.
8. Griffin, J.S.; Burpee, R.W.; Marks Jr., F.D.; Franklin, J.L. Real-Time Airborne Analysis of Aircraft Data Supporting Operational Hurricane Forecasting. *Wea. Forecasting*. **1992**, *7*, 480–490. DOI:10.1175/1520-0434(1992)007<0480:RTAAOA>2.0.CO;2.
9. Wood, V.T.; Brown, R.A. Effects of Radar Proximity on Single-Doppler Velocity Signatures of Axisymmetric Rotation and Divergence. *Mon. Wea. Rev.* **1992**, *120*, 2798–2807. DOI:10.1175/1520-0493(1992)120<2798:EORPOS>2.0.CO;2.
10. Wood, V.T. A Technique for Detecting a Tropical Cyclone Center Using a Doppler Radar. *J. Atmos. Ocean. Technol.* **1994**, *11*, 1207–1216. DOI:10.1175/1520-0426(1994)011<1207:ATFDAT>2.0.CO;2.
11. Willoughby, H.E.; Chelmow, M.B. Objective Determination of Hurricane Tracks from Aircraft Observations. *Mon. Wea. Rev.* **1982**, *110*, 1298–1305. DOI:10.1175/1520-0493(1982)110<1298:ODOHTF>2.0.CO;2.
12. Dodge, P.; Burpee, R.W.; Marks Jr., F.D. The Kinematic Structure of a Hurricane with Sea Level Pressure Less Than 900mb. *Mon. Wea. Rev.* **1999**, *127*, 987–1004. DOI:10.1175/1520-0493(1999)127<0987:TKSOAH>2.0.CO;2.
13. Marks, F.D.; Houze, R.A.; Gamache, J.F. Dual-Aircraft Investigation of the Inner Core of Hurricane Norbert. Part I: Kinematic Structure. *J. Atmos. Sci.* **1992**, *49*, 919–942. DOI:10.1175/1520-0469(1992)049<0919:DAIOTI>2.0.CO;2.
14. Farnebäck, G.; Motion, T.-F. Estimation Based on Polynomial Expansion. In *Proceedings of the 13th Scandinavian Conference on Image Analysis (SCIA), Halmstad, Sweden*, 2003, 29 June.
15. Chang, P.-L.; Jong-Dao Jou, B.J.-D.; Zhang, J. An Algorithm for Tracking Eyes of Tropical Cyclones. *Weather Forecasting*. **2009**, *24*, 245–261. DOI:10.1175/2008WAF2222112.1.
16. Lee, W.-C.; Marks Jr., F.D. Tropical Cyclone Kinematic Structure Retrieved from Single-Doppler Radar Observations. Part Ⅱ: The GBVTD-Simplex Center Finding Algorithm. *Mon. Wea. Rev.* **2000**, *128*, 1925–1936. DOI:10.1175/1520-0493(2000)128<1925:TCKSRF>2.0.CO;2.